JOURNAL OF CHEMICAL INFORMATION AND MODELING

Article

pubs.acs.org/jcim

Investigation on the Effect of Key Water Molecules on Docking Performance in CSARdock Exercise

Ashutosh Kumar and Kam Y. J. Zhang*

Zhang Initiative Research Unit, RIKEN, 2-1 Hirosawa, Wako, Saitama 351-0198, Japan

ABSTRACT: Water molecules are routinely included in molecular docking methods and protocols because of their important role in mediating ligand protein interactions. However, it is still unclear that the inclusion of explicit water molecules improves docking accuracy. To explore the effect of including key water molecules on docking accuracy and performance, we participated in the CSARdock 2011 benchmark exercise. This exercise provides a valuable opportunity for researchers to test their docking programs, methods, and protocols in a blind testing environment. The benchmark exercise and its analysis presented in this paper showed that the performance of current docking programs can be improved by incorporating carefully selected water molecules. Our study showed that water mapping calculations can be used to select key water molecules from experimentally identified water positions for molecular dockings. We have observed that inclusion of all binding site water molecules led to reduced performance and erroneous results. Moreover, an overall improvement in binding pose prediction was achieved when computationally selected water molecules are included during docking simulations. The improvement in the docking performance by including water molecules also depends on protein system, chemical class of ligand, docking method, and scoring function.

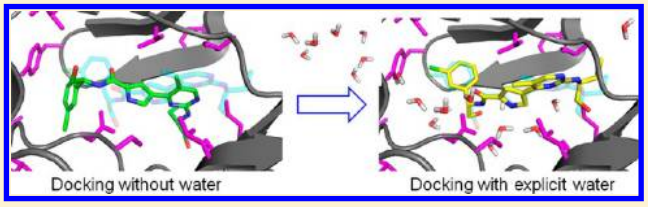

INTRODUCTION

Water molecules constitute the physiological environment for the interaction of biomolecules. Specifically, water molecules play an important role in mediating interactions of proteins with their ligands by forming a hydrogen bond network.[1−3] An analysis of 392 protein complex crystal structures revealed the presence of at least one bridging water molecule at the protein−ligand interface in more than 85% of cases.[4] On average, there were 3.5 bridging water molecules making polar interactions with both protein and ligand.[4] Binding of ligands generally involves the displacement of binding site water molecules, and the ligand has to overcome this desolvation penalty by forming favorable interactions.[5] Although many solvent molecules are easily displaceable, some water molecules are tightly held. The displacement of tightly bound water molecules may drastically weaken the binding of ligands that displace them.[6−8]

Molecular docking is a routinely used computational approach to study protein ligand interactions. Over the past two decades, there has been significant development in docking protocols, algorithms, and scoring functions.[9−11] Due to the importance of water molecules in protein−ligand interactions, many programs take into account of water in molecular docking simulations. The most common approach is by using continuum solvation models.[12−15] There are also many reported studies that include explicit water molecules in docking.[16−20] Some of these studies showed an improvement in the docking accuracy by considering all crystallographic water molecules in the binding site.[16,17,20] However, this may lead to bias toward the native binding pose as it limits the number of possible binding modes.[21] Other studies reported that the use of selected water molecules resulted in improved docking performance.[22,23] In these studies, water molecule sites found in multiple crystal structures (of the same protein or structurally related proteins) were chosen for inclusion in docking. However, this approach demands careful selection because sometimes water molecules in crystal structures may be just artifacts especially in low resolution crystal structures.[24−26] The requirement for many crystal structures is a constraint in such type of selection. Moreover, this approach is not appropriate in the case of comparative or de novo modeled structures which include no water molecules. Under these circumstances, computational methods are indispensable for predicting the location and orientation of binding site water molecules.

Over past few years, many methods for predicting water positions have been developed.[27−29] These include molecular dynamics or Monte Carlo simulation based methods in explicit water environment. These methods predict water positions by either averaging water molecule locations or by taking peaks in a density function.[30] One of the molecular dynamics based methods is WaterMap.[31−34] It exploits explicit solvent molecular dynamics simulation with statistical thermodynamic analysis of water clusters to predict the location of tightly bound water molecules. JAWS[35] is another method that uses a Monte Carlo simulation and statistical thermodynamics methodology to predict water location in protein ligand binding site. Since molecular dynamics or Monte Carlo based methods are computationally expensive, fast solvation based

Special Issue: 2012 CSAR Benchmark Exercise

Received: November 30, 2012

   dx.doi.org/10.1021/ci400052w | J. Chem. Inf. Model. XXXX, XXX, XXX−XXX

methods have been developed in order to quickly predict water positions. GRID[36,37] uses a water probe to calculate its interaction energy with the protein. SZMAP[38] uses a semicontinuum approach to predict water positions and orientations in proteins especially at ligand binding sites. SZMAP uses a single explicit water molecule with Poisson−Boltzmann continuum solvent method to estimate various thermodynamic properties. Ross et al.[27] developed a method WaterDock which accurately predicts water locations by docking water molecules using Autodock-Vina.[39]

Recently, some docking methodologies have been developed that include water molecules "on the fly" during the docking process. These methodologies simultaneously predict water positions as well as binding poses of ligands. One such method is the force field and hydration docking method developed by Forli and Olson.[40] The hydrated docking method reported substantial improvement in docking performance by predicting water locations during docking. Lie et al.[41] reported another methodology implemented in docking program Molegro Virtual Docker[42] to predict water positions and docking of ligands at the same time. In this methodology, solvated ligands are docked and water molecules are retained or displaced depending on energetic contributions during molecular docking. Methodologies performing hydrated docking show promise in identifying key interacting water molecules in protein ligand binding sites. However, these methods need to be improved further to become generally useful. At present, a good strategy for identifying favorable water locations and orientations is to follow a consensus approach by complementing experimentally identified water positions with computationally identified positions. Computational approaches such as SZMAP can be used to identify key crystallographic water molecules based on water thermodynamics in binding site.

CSARdock 2011 benchmark exercise is a blind assessment which researchers can use to test their docking methods, protocols, and programs. The data set for CSARdock 2011 benchmark exercise included unpublished crystal structures and affinity data for four targets: checkpoint kinase 1 (CHK1), extracellular signal regulated kinase 2 (ERK2), UDP-3-*O*-(*R*-3-hydroxymyristoyl)-GlcNAc deacetylase (LpxC), and Urokinase provided by Abott, Vertex, and CSAR. In order to evaluate the effect of including key water molecules on RosettaLigand[43−45] docking performance, we participated in the CSARdock 2011 benchmark exercise. Here we describe the results obtained from blind docking of the benchmark data set both with and without key water molecules. We report an analysis of our strategy to explore factors that affect the performance of our protocol.

MATERIALS AND METHODS

By participating in the CSARdock 2011 benchmark exercise, we have explored the role of key water molecules in protein ligand docking using the flexible docking program RosettaLigand. We have carried out two sets of docking experiments (a) RD-NW RosettaLigand docking without water molecules and (b) RD-PW RosettaLigand docking with computationally predicted and selected key water molecules. The detailed methodology used for docking calculation is as follows:

Data Set. Two data sets (1) CSARdock 2011 benchmark exercise data set and (2) full CSARdock data set were used to test our approach. CSARdock 2011 benchmark exercise data set consists of four proteins CHK1, ERK2, LpxC, and Urokinase with 47, 39, 16, and 20 compounds, respectively. This data was used for testing our docking approach in a blind testing environment. A full CSARdock data set consists of additional compounds and inhibitory activities for CHK1, ERK2, LpxC, and Urokinase. It also contains two additional proteins CDK2 and CDK2-CyclinA with their actives and experimentally tested decoys. This data set was used to carry out retrospective analysis of our approach that led to substantial improvements.

Water Mapping Calculation using SZMAP. Water mapping program, SZMAP[38] was used to predict the regions which are favorable for water. SZMAP uses a semicontinuum approach[46−48] that combines single explicit water molecule with Poisson−Boltzmann continuum solvent method. SZMAP places a single explicit water molecule at each grid point and estimates various thermodynamic properties by treating the rest as continuum. The grid spacing of 0.5 Å was used to carry out SZMAP calculations. SZMAP samples orientations of water molecule while it interacts with continuum solvent and with protein and ligand molecules. All the crystal water molecules were removed before running SZMAP calculations. The REDUCE program[49] was used to optimize the positions of protein hydrogens before running SZMAP calculations. The input files for running SZMAP calculations were prepared using the *pch* utility. It adds amberFF94 partial charges for protein, formal charges on the ions, and *am1bcc* charges on ligands. SZMAP results were visualized using SZMAP extensions in VIDA.[50] The selection of key water molecules for CSARdock 2011 benchmark exercise was achieved by overlaying SZMAP results on crystal structures. In this study, SZMAP was used to identify key water molecules that are important for ligand binding among all the crystallographic waters. It is important to note that, instead of determining the water positions "dynamically" or "ab initio", we followed the consensus approach. We complemented the experimentally identified positions with computational calculation of water thermodynamics. Here, SZMAP was used to identify key crystallographic waters among the crystallographic waters determined experimentally. In this way, we take advantage of the fact that crystallographic water information is available for all the protein targets in the CSARdock exercise.

Preparation of Ligand and Receptor Structures for Molecular Docking. Preparation of receptor structures for docking was accomplished using MOE2011.10.[51] PDB codes 2E9N, 3I5Z, 3P3E, 1OWE, 3QQF, and 3MY5 were used to carry out docking for CHK1, ERK2, LpxC, Urokinase, CDK2, and CDK2-CyclinA, respectively. To prepare, receptor structures for molecular docking hydrogens were added and bond orders were assigned. All water molecules except the key water molecules and atoms of the inhibitor were removed. The protonation state of charged residues were determined and implemented using Protonate3D in MOE2011.10. LpxC contains a Zn^{2+} ion that coordinates with inhibitors and His78 and His237 in the binding site.[52] This Zn^{2+} ion was retained for docking and default Zn^{2+} ion parameters (as implemented RosettaLigand) were used. RosettaLigand handles the flexibility of a ligand by using a set of diverse ligand conformations; therefore, a conformational ensemble for each ligand in both the CSARdock data sets was generated using OMEGA.[53] Partial charges to ligands were assigned according to the AM1BCC semiempirical method.[54]

Molecular Docking and Scoring. All the molecular dockings were achieved using RosettaLigand.[43−45] RosettaLigand is a fully flexible receptor and ligand docking program. It employs stochastic conformational search to identify low-energy protein ligand complexes. The docking procedure in

dx.doi.org/10.1021/ci400052w | J. Chem. Inf. Model. XXXX, XXX, XXX−XXX

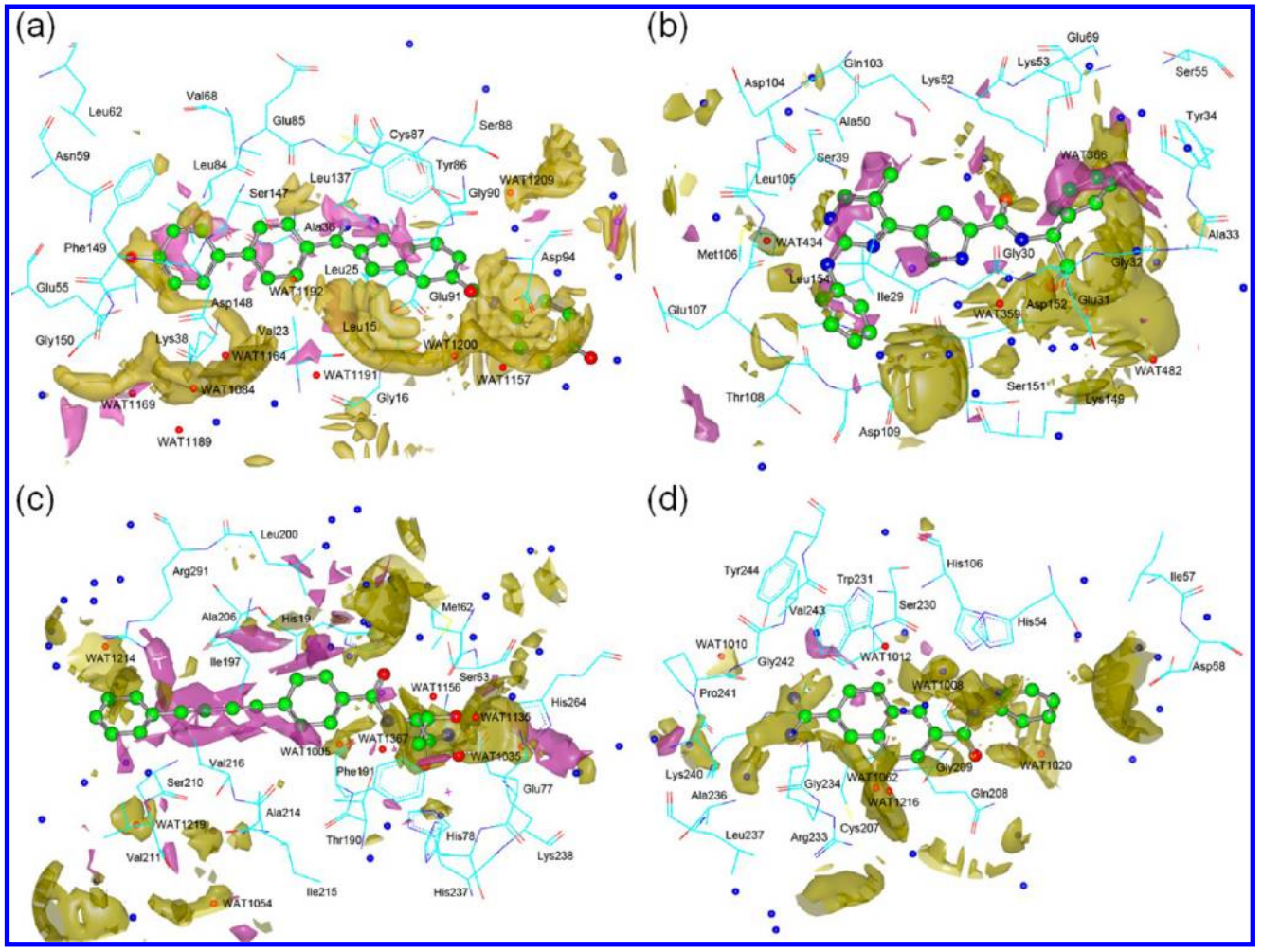

Figure 1. SZMAP results for all four proteins: (a) CHK1, (b) ERK2, (c) LpxC, (d) Urokinase. Red spheres represent water included in docking while blue spheres represent other active site waters. The yellow contour represents regions favorable for water binding while the purple contour represents unfavorable regions.

RosettaLigand starts with placement of each ligand conformation from ensemble to receptor binding site. Side-chain amino acid rotamer conformations are then placed around the ligand and optimized using a Metropolis Monte Carlo simulated annealing algorithm. To rank docking poses, RosettaLigand uses an energy function that contains van der Waals attractive and repulsive forces, electrostatic interactions, solvent effects, hydrogen bonding, and empirically derived torsion potentials.[43−45] We generated approximately 5000 docked poses for each ligand and each receptor. The top-scoring 5% were reranked by ligand−protein interface scores (InterfaceDelta term in RosettaLigand scores) which is the difference in the energy of protein in ligand bound and unbound state. The main objective of this research was to address the question how key crystallographic waters can improve docking performance. Hence, all the molecular docking calculations were performed in the presence or absence of crystallographic water molecules for comparison. The crystallographic water molecules in molecular docking were kept fixed. This is contrary to the concept of flexible docking where the water molecules should be determined dynamically and be allowed to move during docking. It is indeed paradoxical to have the position of key water molecules fixed in a "flexible" docking exercise. However, it is challenging to allow full flexibility to water molecules during docking. It may be more necessary to allow some flexibility or to refine the positions if the water molecules were predicted computationally. However, with crystallographic water molecules available in the target structure, it is more practical to use their crystallographic positions. Without an established and proven procedure of allowing flexible water molecules during docking, we have chosen to fix the water position in our protocol for practical reasons. The molecular docking calculations were performed on 97.4 TFLOPS Intel Xeon 5570 based Massively Parallel PC Cluster of RIKEN Integrated Cluster of Clusters (RICC). The computation time to generate 5000 docked poses utilizing maximum of 200 ligand conformations was approximately 40 h on 4 CPUs depending upon the protein−ligand complex.

RESULTS AND DISCUSSION

Identification of Key Water Molecules. Our approach is based on previous observations that inclusion of water molecules in docking improves the docking accuracy. It has been observed that inclusion of all active site water molecules creates bias for ligands of a particular chemical class and may not work for others. Also, sometimes water positions are not reliable in crystal structures, especially in structures of low resolution.[24−26] Therefore, the appropriate selection of water molecules to be included in docking studies is crucial. Several

dx.doi.org/10.1021/ci400052w | J. Chem. Inf. Model. XXXX, XXX, XXX−XXX

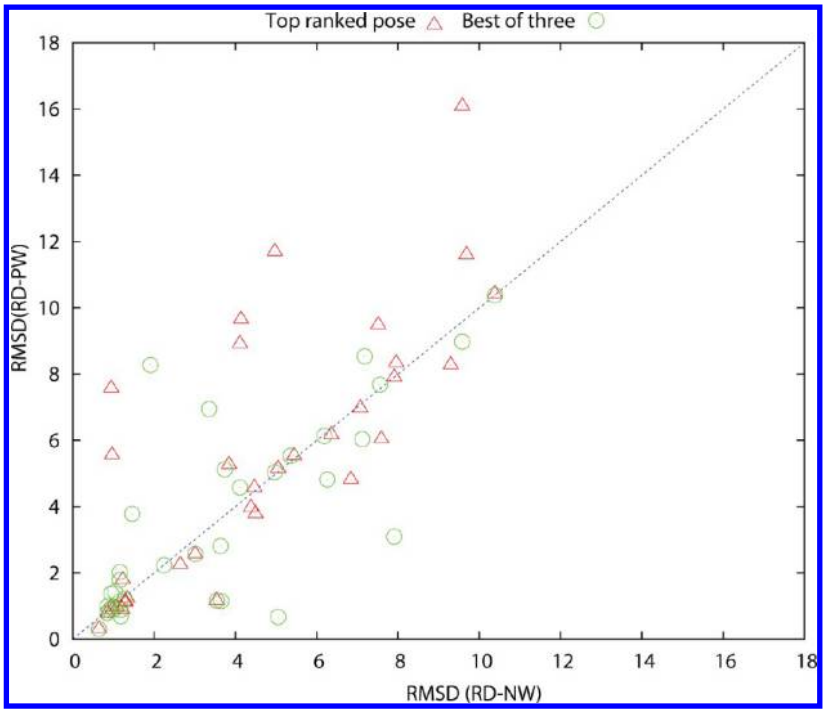

Figure 2. Scatterplot of RMSD in 34 crystal structures with docking poses generated using RD-NW and RD-PW for CHK1, ERK2, LpxC, and Urokinase inhibitors of the CSARdock 2011 benchmark exercise data set. The RMSD values are presented in angstroms.

computational methods exist that evaluate solvent energetics for the identification of key water molecules. In this study, key water molecules for each protein target were identified by running water mapping calculation with SZMAP[38] using the protocol mentioned previously.

Water mapping calculations were performed on the binding pockets of CSARdock 2011 benchmark exercise data set proteins CHK1 (PDB code 2E9N[55]), ERK2 (PDB code 3I5Z[56]), LpxC (PDB code 3P3E[52]), and Urokinase (PDB code 1OWE[57]). The results of water mapping calculations are presented in Figure 1 for all four data set proteins. Results represent neutral difference free energies, which is the difference of free energy between water and uncharged water. Neutral difference free energies map the polarity within the binding pocket and are represented as colored contours in Figure 1. The yellow contour represents the region favorable for water binding (negative neutral difference free energy), and the purple contour represents the region unfavorable for water binding (positive neutral difference free energy). As shown in Figure 1, water mapping calculation identified both the favorable and unfavorable regions for water binding. The ligand in three proteins (CHK1, ERK2, and LpxC) displace region with both yellow and purple contour while ligand in Urokinase displaces only regions with negative neutral difference free energies. Polar and nonpolar functional groups in ligands overlap well with the neutral difference free energy contours. As we have previously mentioned, a good approach for identifying water position is to follow an integrative approach by combining computational results with crystal structure water molecules. Neutral difference free energy grid contours can be used to select key water molecules for docking calculations. An analysis of crystal structures of CHK1, ERK2, LpxC, and Urokinase revealed the presence of 25, 39, 48, and 28 water molecules in the binding site, respectively. Overlay of yellow contours, i.e. the favorable regions for binding of water molecules with active site water molecules, lead to the selection of 9, 4, 8, and 6 water molecules for CHK1, ERK2, LpxC, and Urokinase respectively. These water molecules are shown as red spheres in Figure 1, while the discarded water molecules are shown as blue spheres.

CSARdock 2011 Benchmark Exercise Blind Predictions. The CSARdock 2011 benchmark exercise data set was prepared as described previously in the manuscript. The inhibitors contained in the data set of CHK1, ERK2, LpxC, and Urokinase were docked to their respective proteins following two docking strategies: RD-NW and RD-PW (see details in Materials and Methods). Docking was carried out using RosettaLigand[43−45] which considers full ligand and protein flexibility. Initially, for each ligand in the data set, 5000 docked poses were generated which were ranked by the RosettaLigand energy function.[43−45] Then, the top 5% of best scoring structures were reranked by ligand−protein interface scores. Finally, the top three poses were selected as the best docked structures and submitted for evaluations. As our goal was to explore docking performance in an unbiased manner therefore, all dockings were conducted in completely blind environment without incorporation of any human knowledge.

In the CSARdock 2011 benchmark exercise, the docking methods were evaluated for generating an accurate pose as well as for ranking of actives over inactive compounds. For this purpose, previously unpublished inhibitor activity data and crystal structures for some of the protein−inhibitor complexes was released to the CSARdock 2011 benchmark exercise participants. On the basis of the inhibitory activity data and crystal structures, performance of RD-NW and RD-PW was measured by two criteria: (1) The first was root mean square deviation (RMSD) of ligand docking poses with corresponding X-ray crystal structure. Heavy atoms of ligands were used to calculate RMSD values using *rmsd.py* script from Schrodinger.[58] (2) Enrichment of actives over inactives was analyzed as a measure to judge docking performance. This was quantified by the area under curve (AUC) of its receiver operating

dx.doi.org/10.1021/ci400052w | J. Chem. Inf. Model. XXXX, XXX, XXX−XXX

characteristic (ROC) plot. The ROC plot is constructed by using a ranked list of CHK1, ERK2, LpxC, and Urokinase inhibitors arranged in order of increasing RosettaLigand Interface Delta. The ROC plot is a plot of sensitivity (how many true positives are retrieved) versus specificity (how many false positives are retrieved) calculated at each position by assuming that all compounds ranked higher as active. The AUC and ROC plots were calculated using the pROC package[59] of R program.[60]

CSAR provided 34 inhibitor bound crystal structures of CSARdock 2011 benchmark exercise data set proteins (14, 12, 4, and 4 for CHK1, ERK2, LpxC, and Urokinase, respectively). These crystal structures were used to evaluate performance of RD-NW and RD-PW by RMSD comparisons. The top three docked poses of few CHK1, ERK2, LpxC, and Urokinase inhibitors in the CSARdock 2011 benchmark exercise data set were first aligned with their respective crystal structures. The alignment facilitates the computation of RMSD with the CSARdock 2011 benchmark exercise data set ligand bound crystal structures. Figure 2 reports the scatterplot of RMSD of ligand poses docked using RD-NW and RD-PW with the crystal structures. Table 1 reports the success rate (%) in reproducing crystal structure conformation within 2 and 2.5 Å. As shown in Figure 2 and Table 1 that when using 2 Å as success criteria, RD-NW and RD-PW could achieve only the success rate of 32.35% and 29.41% when top ranked posed was used for RMSD calculation. However, when best of the three poses was used for RMSD calculation success rate slightly improved to 44.12% for both RD-NW and RD-PW, respectively. There were no significant changes in success rates even with more flexible success criteria of 2.5 Å RMSD. Moreover, no improvement in docking performance was observed while using explicit water molecules (Figure 2 and Table 1).

Table 1. Success Rate of CSARdock Benchmark Exercise Docking with RD-NW and RD-PW

		% of inhibitor within 2 Å (top ranked pose)		% of inhibitor within 2 Å (best of three)	
proteins	number of inhibitors	RD-NW	RD-PW	RD-NW	RD-PW
CHK1	14	21.4	21.4	28.5	35.7
ERK2	12	33.3	25	50	50
LpxC	4	50	50	75	50
Urokinase	4	50	50	50	50
total	**34**	**32.35**	**29.41**	**44.12**	**44.12**
		% of inhibitor within 2.5 Å (top ranked pose)		% of inhibitor within 2.5 Å (best of three)	
proteins	number of inhibitors	RD-NW	RD-PW	RD-NW	RD-PW
CHK1	14	21.4	21.4	28.5	35.7
ERK2	12	33.3	25	50	50
LpxC	4	50	50	75	75
Urokinase	4	50	75	75	75
total	**34**	**32.35**	**32.35**	**47.06**	**50**

The ranking efficiency of RD-NW and RD-PW docking strategies was measured by estimating the AUC of the ROC plot. The AUC measures how high a randomly selected active compound is ranked compared to a randomly chosen inactive compound. The AUC values were calculated for CHK1, LpxC, and Urokinase only as inactive compounds for ERK2 were not present in CSARdock 2011 benchmark exercise data set. Figure 3 shows the ROC plot which is constructed by using a ranked list of CSARdock 2011 benchmark exercise data set (both active and inactive compounds) arranged in order of increasing docking score. The enrichment of actives was almost random in the case of both RD-NW and RD-PW in with AUC values of 0.546 and 0.549 for CHK1 and 0.531 and 0.562 LpxC, respectively. Although, the enrichment was better for Urokinase inhibitors with AUC values of 0.812 and 0.812 for RD-NW and RD-PW respectively, but there was very little difference between two docking approaches.

Retrospective Analysis Using Full CSARdock Data Set. As discussed in the previous section, no significant improvement in the docking performance was observed after including the key water molecules selected using water mapping calculation. The performance of docking remains the same and the procedure could not accurately dock more than 50% of CSARdock 2011 benchmark exercise compounds. This was contrary to our expectations as we anticipated an improvement by including key water molecules. The possible reasons for inferior performance of docking with key water molecules may be the following: (1) *Selection of key water molecules*: In the CSARdock benchmark exercise, we selected key water molecules from SZMAP calculations by overlaying the SZMAP grids on crystal structure water molecules. It is a brute force approach where it is easy to miss one or two important water molecules. (2) *Scoring function*: RosettaLigand[43−45] generates a huge number of poses which are ranked first by Rosetta energy function and then by ligand−protein interaction score. Therefore, it is possible that native binding pose is not the best pose or among the top three poses.

To bootstrap the shortcomings in our docking approach, we first validated the ability of SZMAP to predict crystallographic water molecules. Generally, the assessment of methodologies predicting water positions requires the reproduction of crystallographic water positions. This type of validation is challenging in the case of SZMAP which places a water molecule at each grid point of the 0.5 Å grid to calculate various thermodynamic properties. A favorable water position can be selected using a particular cutoff of free energy differences between water and uncharged water (neutral difference free energies in SZMAP). The determination of energy cutoff is critical for the selection of favorable water positions and requires detailed investigation. To access SZMAP's ability to accurately reproduce crystallographic water positions, we have used a slightly different approach. As the aim of this research was to identify key water molecules, we focused on the water molecules that were retained or displaced during ligand binding. The validation study was performed using four apo and holo proteins from the data set used by Ross et al.[27] The data set comprising eight crystal structures is shown in Table 2. We ran SZMAP calculations on apo structures and checked whether the water molecule which was predicted to have positive or near zero neutral difference free energy is displaced by ligand in the holo structure. We also checked whether the water molecule predicted to have highly negative neutral difference free energy is actually replaced by polar functional group of ligand to compensate for desolvation penalty. SZMAP calculations were performed on binding site water position using "at_coords" option of SZMAP. The water molecules in apo structures that are within 5 Å of any ligand atom (when apo and holo structures are superimposed) were considered as

dx.doi.org/10.1021/ci400052w | J. Chem. Inf. Model. XXXX, XXX, XXX−XXX

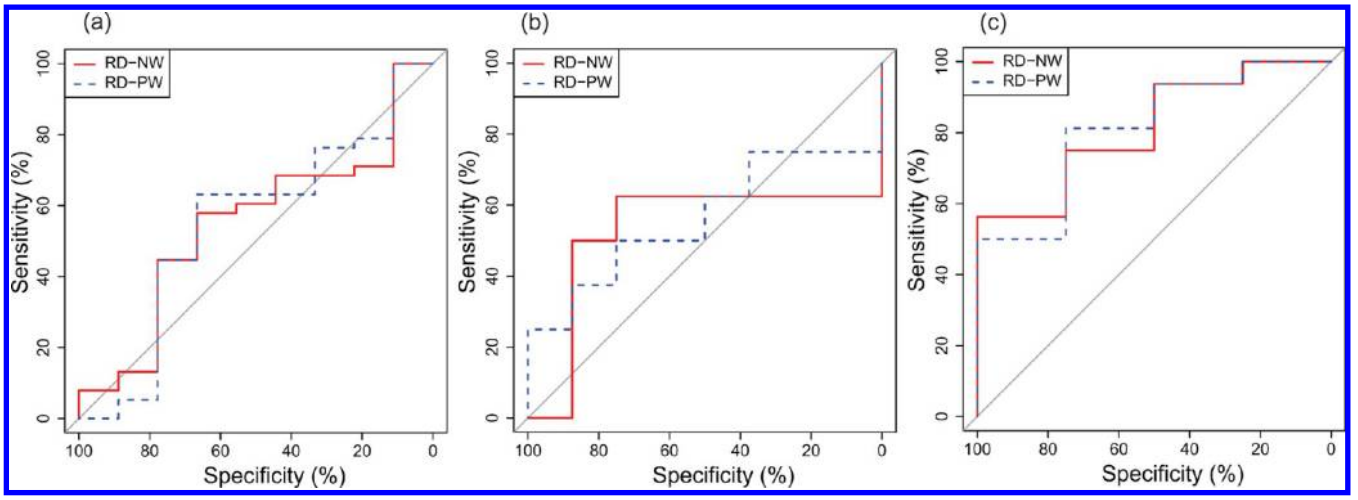

Figure 3. Ranking efficiency of RD-NW and RD-PW on CSARdock 2011 benchmark exercise data set (a) CHK1, (b) LpxC, and (c) Urokinase.

Table 2. Apo and Holo Protein Structures Used for the Validation of SZMAP Prediction

protein	ligand	PDB code	resolution (Å)
BRD4	none	2OSS	1.35
BRD4	JQ1	3MXF	1.6
trypsin	none	1S0Q	1.02
trypsin	BEN	1BTY	1.5
HSP90	none	1AH6	1.8
HSP90	ADP	1AM1	2
penicillopepsin	none	3APP	1.8
penicillopepsin	PP8	1BXQ	1.41

binding site waters. Figure 4 reports the neutral difference free energies obtained by running SZMAP calculations on binding site water coordinates of BRD4, trypsin, HSP90, and penicillopepsin proteins. The positive neutral difference free energy represents undesirable water position, while the negative neutral difference free energy represents the tightly bound water. The water molecules in apo structures that are within 1 Å of any ligand atom (when apo and holo structures are superimposed) were considered as displaced water molecules. For BRD4, trypsin, HSP90, and penicillopepsin proteins, 5, 4, 8, and 5 water molecules respectively were displaced by corresponding ligands to bulk water (shown as blue circles in Figure 4). In a majority of the cases, water molecules with positive or near zero neutral difference free energy in apo structures were displaced by a ligand in holo structures (shown as blue circles in Figure 4). SZMAP accurately predicted the displacement of 5, 2, 6, and 4 water molecules in BRD4, trypsin, HSP90, and penicillopepsin, respectively. WAT391 and WAT393 in HSP90 and WAT362 in penicillopepsin were also displaced by ligand despite the fact that they have high negative neutral difference free energy. SZMAP predicted WAT391 and WAT393 in HSP90 and WAT362 in penicillopepsin as highly stable. Therefore, the penalty due to desolvation of these waters need to be overcome by replacement with a polar functional group in the ligand. Indeed, as shown in Figure 5, these water molecules were displaced by functional groups of equivalent properties. The positions of WAT391 and WAT393 in HSP90 binding site were occupied by phosphate oxygen and amine in the adenine core of ADP, respectively. Similarly, SZMAP predicted that a highly stable WAT362 in penicillopepsin is displaced by the phosphate oxygen of ligand (Figure 5). Furthermore, WAT621 in penicillopepsin is predicted to be unstable and was displaced by the nonpolar group (Figure 5).

The results of above validation analysis suggest that SZMAP can accurately identify water positions and properties. We next carried out a retrospective analysis using the full CSARdock data set. This data set was released by CSAR after completion of the CSARdock 2011 benchmark exercise to facilitate retrospective analysis. This data set consists of 59 crystal structures and binding affinities for 343 compounds for CHK1, ERK2, LpxC, Urokinase, CDK2, and CDK2-CyclinA. The data were provided by Abbott Laboratories, Vertex Pharmaceuticals, and CSAR. Full CSARdock data set also included inhibitors and activities for CHK1, ERK2, LpxC, and Urokinase that were absent from the CSARdock 2011 benchmark exercise data set. Apart from this, inhibitors and some experimentally confirmed decoys for CDK2 and CDK2-CyclinA are also included.

In the CSARdock 2011 benchmark exercise we have used neutral free energy difference contours overlaid on crystal structure water to select key water molecules. This approach is little time-consuming as water mapping is performed at the whole binding pocket. Here, instead of running at each grid point within the binding pocket, water mapping calculations were performed only on the crystal structure water coordinates. This gives a quantitative estimate that where water is stabilizing or destabilizing the ligand binding that ultimately led to the selection of key water molecules as shown in Figure 6. Negative neutral difference free energies annotated water molecules (shown as red spheres) represent the positions where water is stabilizing the ligand binding. The locations where water is destabilizing the ligand binding were represented by positive neutral difference free energy annotated water molecules (shown as blue spheres). The cutoff of −1.0 kcal/mol was taken to select waters that stabilize ligand binding. The water molecules failed to meet this cutoff are presented as yellow spheres.

Docking was carried out using three strategies instead of the two used previously in the CSARdock 2011 benchmark exercise: (1) RosettaLigand docking without water molecules (RD-NW), (2) RosettaLigand docking with all binding site X-ray water molecules (RD-XW), and (3) RosettaLigand docking with computationally predicted and selected water molecules (RD-PW). Retrospective analysis was performed in a nonblind environment, but care has been taken to avoid any bias associated with docking. For example, unbound ligand

dx.doi.org/10.1021/ci400052w | J. Chem. Inf. Model. XXXX, XXX, XXX−XXX

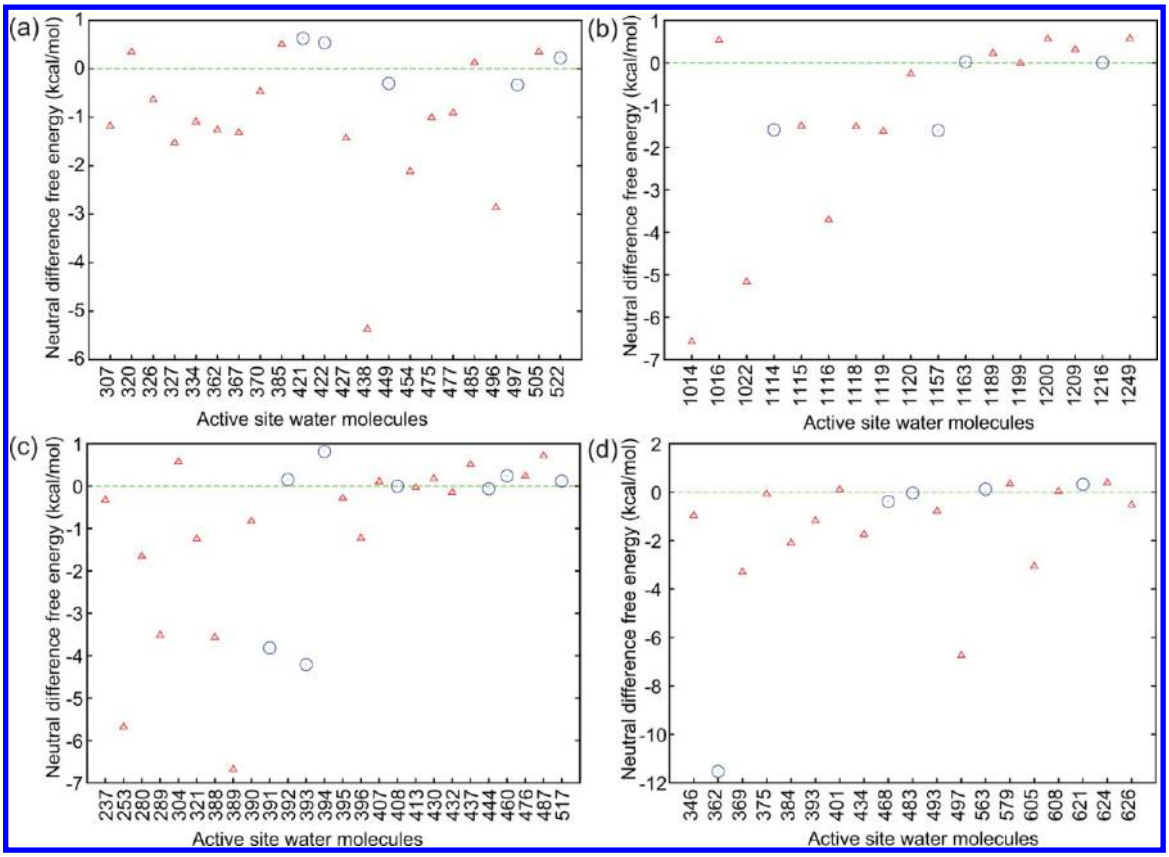

Figure 4. SZMAP predicted neutral difference free energy of binding site waters for (a) BRD4, (b) trypsin, (c) HSP90, and (d) penicillopepsin. Waters displaced by ligands are shown as blue circles.

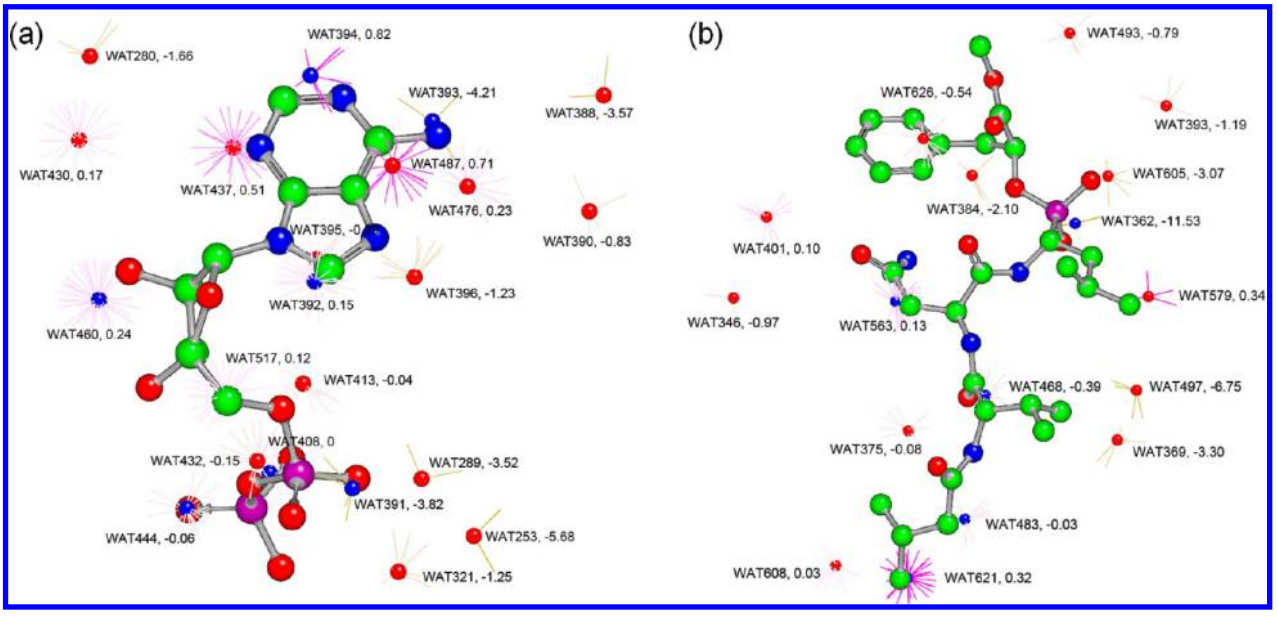

Figure 5. Graphical representation of SZMAP predicted neutral difference free energy of binding site waters. Blue spheres represent crystallographic waters displaced by ligands while the red spheres represent other apo structure water molecules in the binding site. Water molecules are annotated with neutral difference free energy values calculated at coordinates of binding site water. Wireframes on water molecules represent orientations sampled during mapping while colors represent neutral difference free energy value (yellow for highly negative and magenta for highly positive).

structures were used in docking and, docking poses were selected without human intervention, etc. The docking performance was analyzed in a similar manner using two criteria as mentioned previously. The full CSARdock data set contains 57 (excluding one apo and one duplicate crystal structure) inhibitor bound crystal structures (17, 12, 5, 7, 15, and 1 for CHK1, ERK2, LpxC, Urokinase, CDK2, and CDK2-CyclinA, respectively). These structures were used for RMSD comparison with docking poses generated using RD-NW, RD-XW, and RD-PW docking strategies. The results are presented

dx.doi.org/10.1021/ci400052w | J. Chem. Inf. Model. XXXX, XXX, XXX−XXX

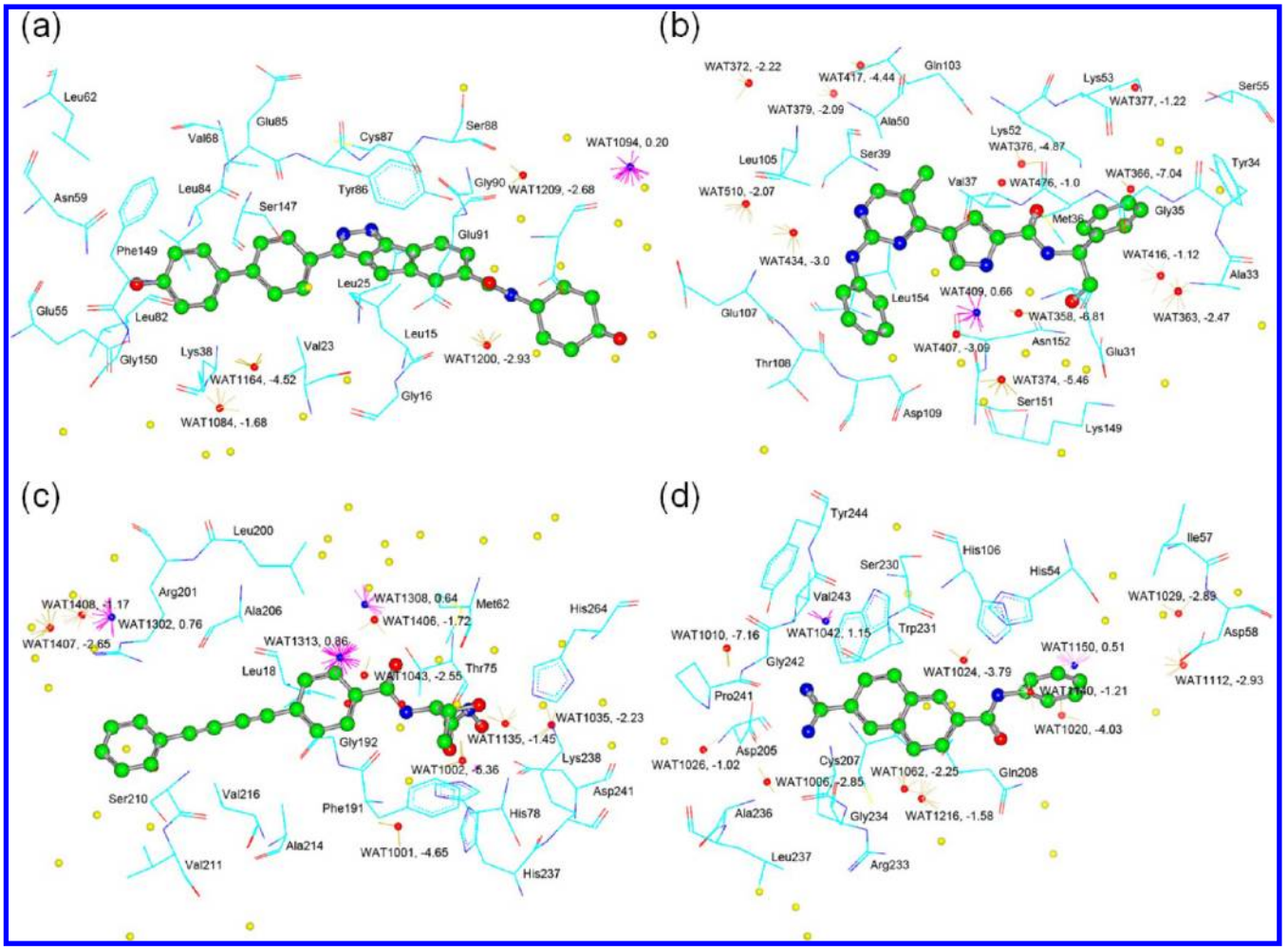

Figure 6. SZMAP water mapping calculations on water coordinates (a) CHK1, (b) ERK2, (c) LpxC, and (d) Urokinase. Red spheres represent waters stabilizing the binding of ligand while blue spheres represent waters destabilizing ligand binding. Yellow spheres represent water molecules in the binding site that do not meet neutral difference free energy cutoff of −1.0 kcal/mol for stabilizing binding.

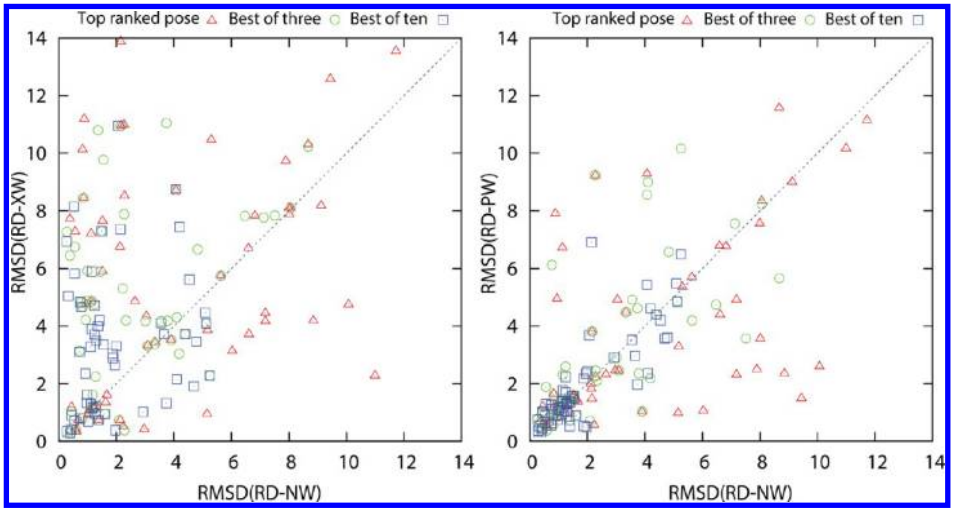

Figure 7. Scatterplot of RMSD in 57 crystal structures with docking poses generated using RD-NW, RD-XW, and RD-PW for CHK1, ERK2, LpxC, Urokinase, CDK2, and CDK2-CyclinA inhibitors of full CSARdock data set. The RMSD values are presented in angstroms.

as a scatter plot (Figure 7) obtained by plotting RMSD values obtained by comparing crystal structures with docked poses. The top ranked pose, top three poses, and top ten poses generated using RD-NW, RD-XW, and RD-PW docking strategies were used for RMSD comparison. Docking success rate (%) was also determined by counting the number of poses within 2 and 2.5 Å RMSD to native and is reported in Table 3.

dx.doi.org/10.1021/ci400052w | J. Chem. Inf. Model. XXXX, XXX, XXX−XXX

Table 3. Success Rate of Docking with RD-NW, RD-XW, and RD-PW[a]

		% inhibitor within 2 Å			% inhibitor within 2 Å			% inhibitor within 2 Å		
		RD-NW			RD-XW			RD-PW		
proteins	number of inhibitors	A	B	C	A	B	C	A	B	C
CHK1	17	23.5	29.4	58.8	23.5	23.5	23.5	35.2	35.2	47.0
ERK2	12	16.6	33.3	41.6	16.6	16.6	25	25	33.3	33.3
LpxC	5	40	80	80	40	40	80	80	80	100
Urokinase	7	42.8	57.1	85.7	85.7	100	100	71.4	71.4	100
CDK2	15	60	80	93.3	0	0	20	46.6	60	86.6
CDK2-CyclinA	1	100	100	100	0	0	0	100	100	100
total	**57**	**36.8**	**52.6**	**70.1**	**24.5**	**26.3**	**36.8**	**45.6**	**50.8**	**66.6**
		% inhibitor within 2.5 Å			% inhibitor within 2.5 Å			% inhibitor within 2.5 Å		
		RD-NW			RD-XW			RD-PW		
proteins	number of inhibitors	A	B	C	A	B	C	A	B	C
CHK1	17	23.5	29.4	58.8	29.4	29.4	35.3	41.2	47.1	64.7
ERK2	12	33.3	50	58.3	16.7	16.7	25	41.7	41.7	41.7
LpxC	5	60	80	80	40	60	80	80	80	100
Urokinase	7	71.4	85.7	85.7	100	100	100	100	100	100
CDK2	15	73.3	93.3	93.3	0	0	26.7	66.7	80	93.3
CDK2-CyclinA	1	100	100	100	0	0	0	100	100	100
total	**57**	**49.1**	**63.2**	**73.7**	**28.1**	**29.8**	**42.1**	**59.6**	**64.9**	**75.4**

[a]A: top ranked pose. B: best of three. C: best of ten.

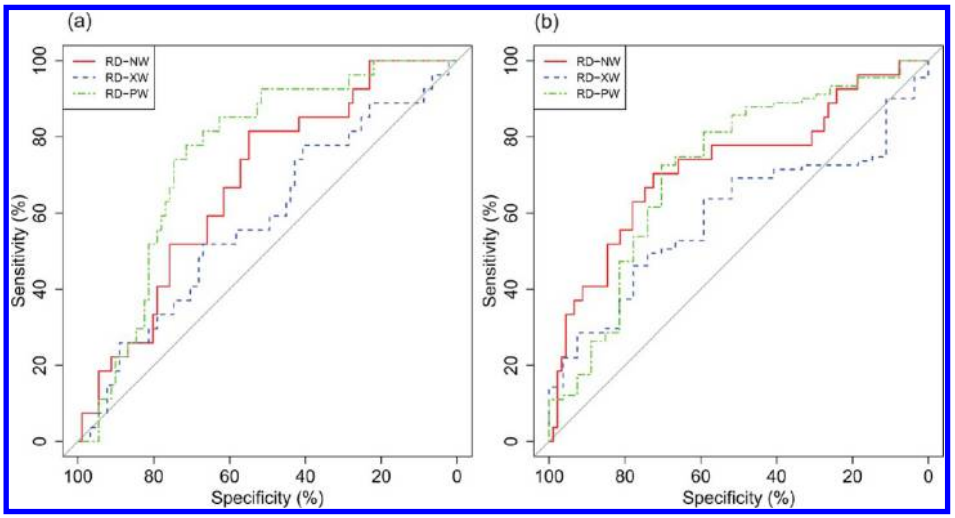

Figure 8. Ranking efficiency of RD-NW, RD-XW, and RD-PW on active and decoys of (a) CDK2 and (b) CDK2-CyclinA of the full CSARdock data set.

As shown in Figure 7, docking by incorporating all active site water molecules (RD-XW) resulted in higher RMSD values and inferior performance as compared with docking without including water molecules (RD-NW). Using 2 Å RMSD as success criteria, success rates were only 24.5, 26.3, and 36.8% for the top ranked pose, best of three, and best of ten, respectively. This could be achieved by using RD-XW docking strategy (Table 3). The performance slightly improved when 2.5 Å RMSD was used as success criteria with success rates of 28.1, 29.8, and 42.1% for top ranked pose, best of three, and best of ten, respectively. However, in the majority of cases, including all active site water molecules reduces docking accuracy. On the other hand, docking by following the RD-PW strategy showed superior performance over RD-NW docking strategy. Incorporation of computationally selected water molecules in dockings resulted in lower RMSD as compared to RD-NW docking strategy where water molecules were not included (Figure 7). As shown in Figure 7, using RD-PW docking, near native poses (within 2.5 Å) were obtained in 59.6% of cases as the top ranking solution as compared to 49.1% while using RD-NW. The superior performance of RD-PW strategy over RD-XW and RD-NW strategies is also reflected in the docking success rates (Table 3). While considering both 2 and 2.5 Å RMSD as success criteria, significant improvement in the docking success rate was achieved for RD-PW. There were 21.38%, 2.68%, and 2.3% improvement in docking success over RD-NW docking strategy for top ranked pose, best of three, and best of ten poses.

The efficiency of ranking actives among RD-NW, RD-XW, and RD-PW docking strategies was then analyzed in similar manner as described for the CSARdock 2011 benchmark exercise. The full CSARdock data set contains active and experimentally tested decoys of CDK2 and CDK2-CyclinA complex. The enrichment of actives over experimentally tested

dx.doi.org/10.1021/ci400052w | J. Chem. Inf. Model. XXXX, XXX, XXX−XXX

decoys of CDK2 and CDK2-CyclinA was estimated by calculating the AUC of the ROC plot. As shown in Figure 8 and Table 4, the RD-XW docking strategy was the worst performer for both the proteins with AUC values of 0.581 and 0.594 for CDK2 and CDK2-CyclinA, respectively. RD-PW docking strategy performed better than RD-NW for CDK2 with AUC value of 0.752 as compared to 0.677 for RD-NW (Figure 8). For CDK2-CyclinA, RD-PW could not perform better than RD-NW, but its performance was on par with RD-NW with AUC values of 0.717 as compared to 0.724 of the RD-NW strategy. Ranking efficiency of three docking strategies for CHK1, LpxC, and Urokinase were estimated similarly using active and inactive compounds, and results are shown in Figure 9 and Table 4. None of the docking strategies were able to discriminate between active and inactive compounds of CHK1 and LpxC and produced AUC values close to random selection. For Urokinase, though all the strategies could discriminate between actives and inactives but there was no improvement when water molecules were included in docking. The AUC values were found to be 0.911, 0.744, and 0.839 for RD-NW, RD-XW, and RD-PW, respectively.

Table 4. AUC Values Obtained by Enrichment Analysis Following RD-NW, RD-XW, and RD-PW Dockings

	number of compounds				
protein	Actives	Inactive/Decoys	RD-NW	RD-XW	RD-PW
CDK2	27	91	0.677	0.581	0.752
CDK2-CyclinA	27	91	0.724	0.594	0.717
CHK1	108	29	0.600	0.582	0.592
LpxC	20	12	0.579	0.445	0.597
Urokinase	36	10	0.911	0.774	0.839

The results of retrospective analysis reveal that docking performance improved when RD-PW strategy was used. The improved performance of RD-PW may be attributed to three reasons: (a) Attractive forces due to water net dipole moment may have caused some ligands (charged ligand) to achieve near native binding poses. This electrostatic attraction may have pulled ligands to form hydrogen bonds with water and guided ligands to near native position. Figure 10 presents two examples where hydrogen bond with water resulted in a docking pose close to the ligand bound crystal structure. As shown in Figure 10a, the formation of a hydrogen bond between WAT1024 and amide nitrogen of a Urokinase ligand (uPa_7) facilitates the ligand to achieve a pose much closer to X-ray crystal structure (RMSD = 0.57). Molecular docking in the absence of key crystallographic water molecules (RD-NW docking strategy) resulted in a pose with RMSD value of 2.23 Å. Similarly, RD-NW strategy was not able to reproduce X-ray crystal structure binding mode of ERK2 ligand (erk000507) and resulted in an RMSD value of 5.15 Å for the top scoring pose (Figure 10b). However, docking including key crystallographic water molecules (RD-PW) predicted a pose close to native ligand with an RMSD value of 0.98 Å for the top ranked pose (Figure 10b). This improvement in performance may be due to hydrogen bonding with WAT359 and WAT476. (b) The presence of key water molecules favor native-like binding mode of ligands. Other binding poses that are far away from the native binding mode may not be possible due to steric clashes with the key crystallographic water molecules. These water molecules are tightly bound to the protein and are not easily replaced by ligands. As illustrated in Figure 10b, spatial arrangement of key crystallographic water molecules guide ligand to nativelike poses. Other binding poses may result in clashes with water for, e.g. with WAT416, WAT362, and WAT407. (c) The formation of crucial hydrogen bond with key crystallographic water is rewarded by the RosettaLigand's scoring function. This is evident from higher docking scores for ligand uPa_7 and erk000507 (−17.13 and −22.47, respectively) using RD-PW as compared to −16.85 and −18.39 using RD-NW docking strategy.

As we have seen in the retrospective analysis using full CSARdock data set, docking performance improved when key water molecules selected using water mapping calculations are included in dockings. But, the same RD-PW approach could not perform well in CSARdock 2011 benchmark exercise. What was the reason for reduced docking performance in CSARdock 2011 benchmark exercise? The results of RMSD analysis of docking poses with crystal structures revealed that below par performance was not the result of RosettaLigand scoring functions as it worked very well in identifying the near native poses if they were among the top ranking poses. In the majority of cases, RosettaLigand scoring approach identified lowest

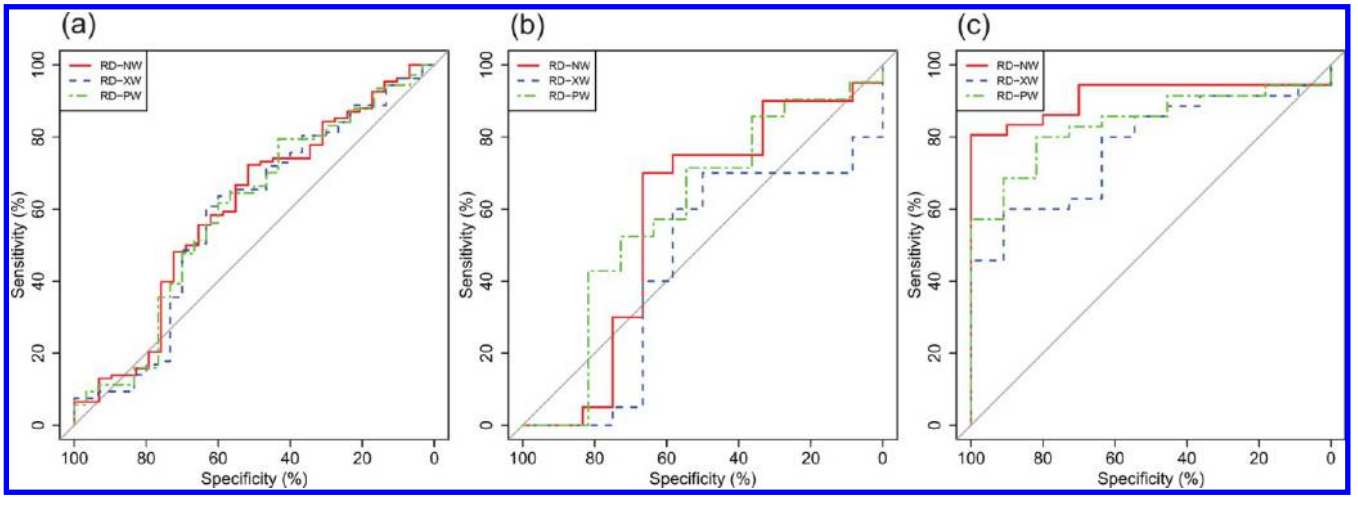

Figure 9. Ranking efficiency of RD-NW, RD-XW, and RD-PW on active and inactives of (a) CHK1, (b) LpxC, and (c) Urokinase of the full CSARdock data set.

dx.doi.org/10.1021/ci400052w | J. Chem. Inf. Model. XXXX, XXX, XXX−XXX

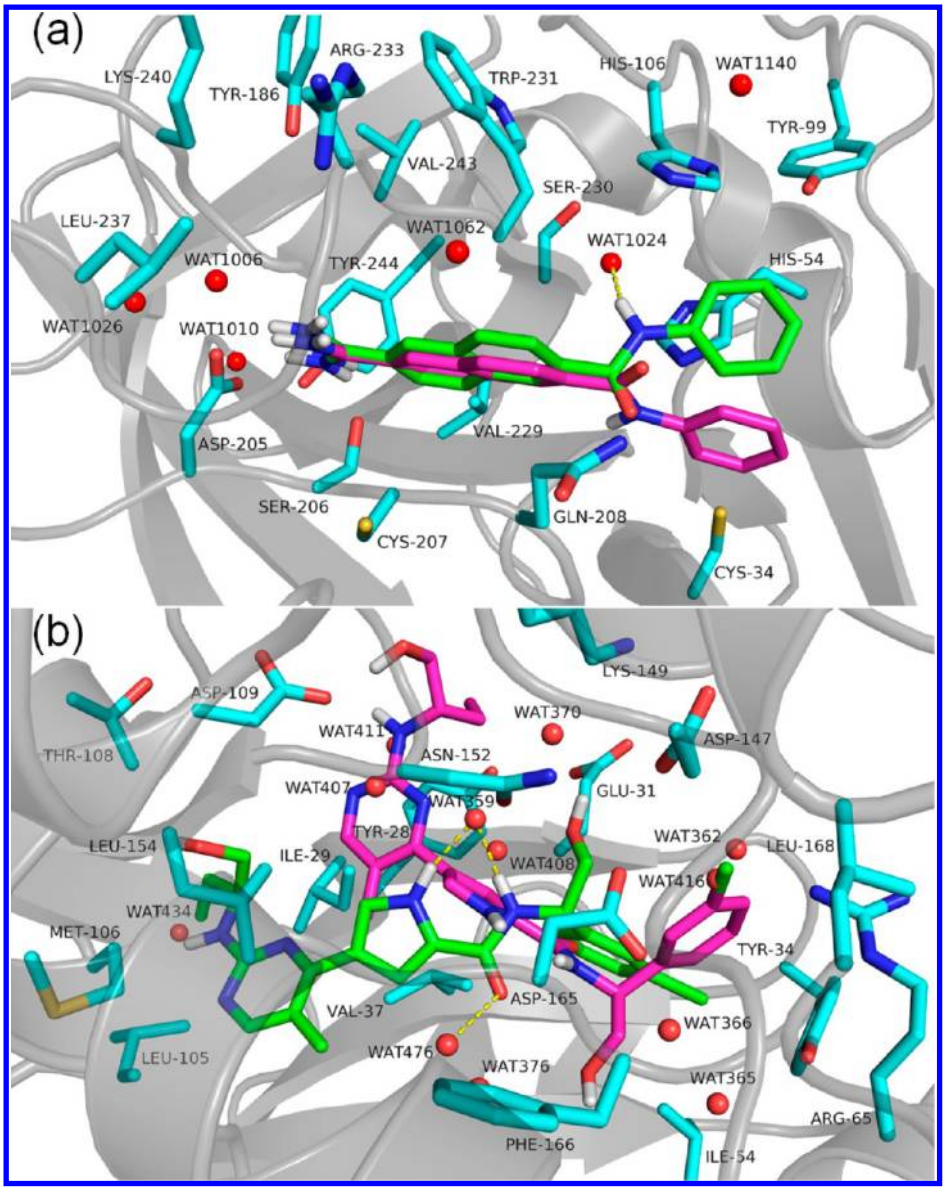

Figure 10. Hydrogen bonding with water governs the generation of near native pose. (a) Urokinase ligand "uPa_7" and (b) ERK2 ligand "erk000507". Magenta and green atom color represents top ranked poses obtained using RD-NW and RD-PW docking strategy. Water molecules are shown as red spheres, while the hydrogen bonds are represented as yellow dash.

RMSD pose as the top ranked pose and the maximum improvement (about 21%) was observed for top ranked pose. The docking performance enhancement was also not due to the just "any water molecule" as inclusion of all binding site water molecules prevented ligands to dock properly because of clashes and thereby reducing the docking performance. In the CSARdock 2011 benchmark exercise, we selected water molecules by overlaying crystal structure water molecules on SZMAP neutral difference free energy grid contours. Using this approach, we selected 9, 4, 8, and 6 water molecules for CHK1, ERK2, LpxC, and Urokinase, respectively. But as shown in Figure 1, only 7, 6, and 5 water molecules could be overlaid on grids for CHK1, LpxC, and Urokinase, respectively (shown as red spheres). This implies that 2 (WAT1191 and WAT1189), 2 (WAT1367 and WAT1156), and 1 (WAT1012) water molecules for CHK1, LpxC, and Urokinase, respectively, were selected by mistake and might have led to reduced performance in dockings. We have rectified this mistake in retrospective analysis by running water mapping calculations on water coordinates which give a quantitative estimate of neutral difference free energy at a particular water position. Using this approach, water molecules that favor ligand binding can be easily selected and others can be discarded. The new selection approach accurately selected water molecules that occupy the position favorable for ligand binding and finally resulted in improvement in docking performance.

■ CONCLUSION

The CSARdock 2011 benchmark exercise was a great platform for researchers to test their docking methods, protocols, algorithm, and scoring functions in a blind testing environment, using activity data and crystal structures provided by CSAR, Abbott, and Vertex Pharmaceuticals. Our results and associated retrospective analysis indicate that the selection of water molecules to be included in docking should be done very carefully. Approaches predicting water locations and config-

dx.doi.org/10.1021/ci400052w | J. Chem. Inf. Model. XXXX, XXX, XXX−XXX

urations should be used together with experimentally identified water sites to select which water molecules should be retained for docking. In the future, efforts should be focused toward incorporating computationally predicted water molecules in multiple orientations within the active site. Scoring functions that consider water positions and orientation should be explored as routes to higher accuracy in molecular docking.

AUTHOR INFORMATION

Corresponding Author

*E-mail: kamzhang@riken.jp. Phone: +81-48-467-8792. Fax: +81-48-467-8790.

Notes

The authors declare no competing financial interest.

ACKNOWLEDGMENTS

We thank RIKEN Integrated Cluster of Clusters (RICC) at RIKEN for the supercomputing resources used for the study. We thank members of our lab for help and discussions. We thank Prof. Jeremy Tame for proofreading this manuscript. We acknowledge the Initiative Research Unit program from RIKEN, Japan, for funding.

REFERENCES

(1) Mancera, R. L. Molecular modeling of hydration in drug design. *Curr. Opin. Drug Discov. Devel.* **2007**, *10* (3), 275−280.

(2) de Beer, S. B.; Vermeulen, N. P.; Oostenbrink, C. The role of water molecules in computational drug design. *Curr. Top. Med. Chem.* **2010**, *10* (1), 55−66.

(3) Wong, S. E.; Lightstone, F. C. Accounting for water molecules in drug design. *Expert Opin. Drug Discov.* **2011**, *6* (1), 65−74.

(4) Lu, Y.; Wang, R.; Yang, C. Y.; Wang, S. Analysis of ligand-bound water molecules in high-resolution crystal structures of protein-ligand complexes. *J. Chem. Inf. Model.* **2007**, *47* (2), 668−675.

(5) Biela, A.; Khayat, M.; Tan, H.; Kong, J.; Heine, A.; Hangauer, D.; Klebe, G. Impact of Ligand and Protein Desolvation on Ligand Binding to the S1 Pocket of Thrombin. *J. Mol. Biol.* **2012**, *418* (5), 350−366.

(6) Clarke, C.; Woods, R. J.; Gluska, J.; Cooper, A.; Nutley, M. A.; Boons, G.-J. Involvement of Water in Carbohydrate-Protein Binding. *J. Am. Chem. Soc.* **2001**, *123* (49), 12238−12247.

(7) Lam, P.; Jadhav, P.; Eyermann, C.; Hodge, C.; Ru, Y.; Bacheler, L.; Meek, J.; Otto, M.; Rayner, M.; Wong, Y.; et al. Rational design of potent, bioavailable, nonpeptide cyclic ureas as HIV protease inhibitors. *Science* **1994**, *263* (5145), 380−384.

(8) Wissner, A.; Berger, D. M.; Boschelli, D. H.; Floyd, M. B.; Greenberger, L. M.; Gruber, B. C.; Johnson, B. D.; Mamuya, N.; Nilakantan, R.; Reich, M. F.; Shen, R.; Tsou, H.-R.; Upeslacis, E.; Wang, Y. F.; Wu, B.; Ye, F.; Zhang, N. 4-Anilino-6,7-dialkoxyquinoline-3-carbonitrile Inhibitors of Epidermal Growth Factor Receptor Kinase and Their Bioisosteric Relationship to the 4-Anilino-6,7-dialkoxyquinazoline Inhibitors. *J. Med. Chem.* **2000**, *43* (17), 3244−3256.

(9) Bottegoni, G. Protein-ligand docking. *Front. Biosci.* **2011**, *16*, 2289−2306.

(10) Meng, X. Y.; Zhang, H. X.; Mezei, M.; Cui, M. Molecular docking: a powerful approach for structure-based drug discovery. *Curr. Comput.-Aided Drug Des.* **2011**, *7* (2), 146−157.

(11) Yuriev, E.; Agostino, M.; Ramsland, P. A. Challenges and advances in computational docking: 2009 in review. *J. Mol. Recognit.* **2011**, *24* (2), 149−164.

(12) Majeux, N.; Scarsi, M.; Apostolakis, J.; Ehrhardt, C.; Caflisch, A. Exhaustive docking of molecular fragments with electrostatic solvation. *Proteins: Struct., Funct., Bioinf.* **1999**, *37* (1), 88−105.

(13) Zou, X.; Yaxiong; Kuntz, I. D. Inclusion of Solvation in Ligand Binding Free Energy Calculations Using the Generalized-Born Model. *J. Am. Chem. Soc.* **1999**, *121* (35), 8033−8043.

(14) Sitkoff, D.; Sharp, K. A.; Honig, B. Accurate Calculation of Hydration Free Energies Using Macroscopic Solvent Models. *J. Phys. Chem.* **1994**, *98* (7), 1978−1988.

(15) Still, W. C.; Tempczyk, A.; Hawley, R. C.; Hendrickson, T. Semianalytical treatment of solvation for molecular mechanics and dynamics. *J. Am. Chem. Soc.* **1990**, *112* (16), 6127−6129.

(16) de Graaf, C.; Pospisil, P.; Pos, W.; Folkers, G.; Vermeulen, N. P. E. Binding Mode Prediction of Cytochrome P450 and Thymidine Kinase Protein-Ligand Complexes by Consideration of Water and Rescoring in Automated Docking. *J. Med. Chem.* **2005**, *48* (7), 2308−2318.

(17) Roberts, B. C.; Mancera, R. L. Ligand-Protein Docking with Water Molecules. *J. Chem. Inf. Model.* **2008**, *48* (2), 397−408.

(18) Huang, N.; Shoichet, B. K. Exploiting Ordered Waters in Molecular Docking. *J. Med. Chem.* **2008**, *51* (16), 4862−4865.

(19) Santos, R.; Hritz, J.; Oostenbrink, C. Role of Water in Molecular Docking Simulations of Cytochrome P450 2D6. *J. Chem. Inf. Model.* **2009**, *50* (1), 146−154.

(20) Thilagavathi, R.; Mancera, R. L. Ligand-Protein Cross-Docking with Water Molecules. *J. Chem. Inf. Model.* **2010**, *50* (3), 415−421.

(21) Hartshorn, M. J.; Verdonk, M. L.; Chessari, G.; Brewerton, S. C.; Mooij, W. T.; Mortenson, P. N.; Murray, C. W. Diverse, high-quality test set for the validation of protein-ligand docking performance. *J. Med. Chem.* **2007**, *50* (4), 726−741.

(22) Lu, S.-Y.; Jiang, Y.-J.; Lv, J.; Zou, J.-W.; Wu, T.-X. Role of bridging water molecules in GSK3β-inhibitor complexes: Insights from QM/MM, MD, and molecular docking studies. *J. Comput. Chem.* **2011**, *32* (9), 1907−1918.

(23) Corbeil, C. R.; Moitessier, N. Docking Ligands into Flexible and Solvated Macromolecules. 3. Impact of Input Ligand Conformation, Protein Flexibility, and Water Molecules on the Accuracy of Docking Programs. *J. Chem. Inf. Model.* **2009**, *49* (4), 997−1009.

(24) Carugo, O.; Bordo, D. How many water molecules can be detected by protein crystallography? *Acta Crystallogr., Sect. D: Biol. Crystallogr.* **1999**, *55* (2), 479−483.

(25) Davis, A. M.; Teague, S. J.; Kleywegt, G. J. Application and Limitations of X-ray Crystallographic Data in Structure-Based Ligand and Drug Design. *Angew. Chem., Int. Ed.* **2003**, *42* (24), 2718−2736.

(26) Yu, B.; Blaber, M.; Gronenborn, A. M.; Clore, G. M.; Caspar, D. L. D. Disordered water within a hydrophobic protein cavity visualized by x-ray crystallography. *Proc. Natl. Acad. Sci. U.S.A.* **1999**, *96* (1), 103−108.

(27) Ross, G. A.; Morris, G. M.; Biggin, P. C. Rapid and accurate prediction and scoring of water molecules in protein binding sites. *PLoS One* **2012**, *7* (3), e32036.

(28) Imai, T.; Hiraoka, R.; Kovalenko, A.; Hirata, F. Locating missing water molecules in protein cavities by the three-dimensional reference interaction site model theory of molecular solvation. *Proteins: Struct., Funct., Bioinf.* **2007**, *66* (4), 804−813.

(29) Imai, T.; Oda, K.; Kovalenko, A.; Hirata, F.; Kidera, A. Ligand Mapping on Protein Surfaces by the 3D-RISM Theory: Toward Computational Fragment-Based Drug Design. *J. Am. Chem. Soc.* **2009**, *131* (34), 12430−12440.

(30) Henchman, R. H.; McCammon, J. A. Extracting hydration sites around proteins from explicit water simulations. *J. Comput. Chem.* **2002**, *23* (9), 861−869.

(31) Beuming, T.; Che, Y.; Abel, R.; Kim, B.; Shanmugasundaram, V.; Sherman, W. Thermodynamic analysis of water molecules at the surface of proteins and applications to binding site prediction and characterization. *Proteins: Struct., Funct., Bioinf.* **2012**, *80* (3), 871−883.

(32) Snyder, P. W.; Mecinović, J.; Moustakas, D. T.; Thomas, S. W.; Harder, M.; Mack, E. T.; Lockett, M. R.; Héroux, A.; Sherman, W.; Whitesides, G. M. Mechanism of the hydrophobic effect in the biomolecular recognition of arylsulfonamides by carbonic anhydrase. *Proc. Natl. Acad. Sci. U.S.A.* **2011**, *108* (44), 17889−17894.

(33) Abel, R.; Salam, N. K.; Shelley, J.; Farid, R.; Friesner, R. A.; Sherman, W. Contribution of Explicit Solvent Effects to the Binding Affinity of Small-Molecule Inhibitors in Blood Coagulation Factor Serine Proteases. *ChemMedChem* **2011**, *6* (6), 1049−1066.
(34) Higgs, C.; Beuming, T.; Sherman, W. Hydration Site Thermodynamics Explain SARs for Triazolylpurines Analogues Binding to the A2A Receptor. *ACS Med. Chem. Lett.* **2010**, *1* (4), 160−164.
(35) Michel, J.; Tirado-Rives, J.; Jorgensen, W. L. Prediction of the water content in protein binding sites. *J. Phys. Chem. B* **2009**, *113* (40), 13337−13346.
(36) Goodford, P. J. A computational procedure for determining energetically favorable binding sites on biologically important macromolecules. *J. Med. Chem.* **1985**, *28* (7), 849−857.
(37) Wade, R. C.; Clark, K. J.; Goodford, P. J. Further development of hydrogen bond functions for use in determining energetically favorable binding sites on molecules of known structure. 1. Ligand probe groups with the ability to form two hydrogen bonds. *J. Med. Chem.* **1993**, *36* (1), 140−147.
(38) *SZMAP*, version 1.1.0; OpenEye Scientific Software, Inc., Santa Fe, NM, USA, 2012; www.eyesopen.com.
(39) Trott, O.; Olson, A. J. AutoDock Vina: Improving the speed and accuracy of docking with a new scoring function, efficient optimization, and multithreading. *J. Comput. Chem.* **2010**, *31* (2), 455−461.
(40) Forli, S.; Olson, A. J. A force field with discrete displaceable waters and desolvation entropy for hydrated ligand docking. *J. Med. Chem.* **2012**, *55* (2), 623−638.
(41) Lie, M. A.; Thomsen, R.; Pedersen, C. N.; Schiott, B.; Christensen, M. H. Molecular docking with ligand attached water molecules. *J. Chem. Inf. Model.* **2011**, *51* (4), 909−917.
(42) Thomsen, R.; Christensen, M. H. MolDock: A New Technique for High-Accuracy Molecular Docking. *J. Med. Chem.* **2006**, *49* (11), 3315−3321.
(43) Davis, I. W.; Baker, D. RosettaLigand Docking with Full Ligand and Receptor Flexibility. *J. Mol. Biol.* **2009**, *385* (2), 381−392.
(44) Davis, I. W.; Raha, K.; Head, M. S.; Baker, D. Blind docking of pharmaceutically relevant compounds using RosettaLigand. *Protein Sci.* **2009**, *18* (9), 1998−2002.
(45) Meiler, J.; Baker, D. ROSETTALIGAND: Protein−small molecule docking with full side-chain flexibility. *Proteins: Struct., Funct., Bioinf.* **2006**, *65* (3), 538−548.
(46) Rashin, A. A.; Bukatin, M. A. Continuum based calculations of hydration entropies and the hydrophobic effect. *J. Phys. Chem.* **1991**, *95* (8), 2942−2944.
(47) Tanger, J. C.; Pitzer, K. S. Calculation of the thermodynamic properties of aqueous electrolytes to 1000 °C and 5000 bar from a semicontinuum model for ion hydration. *J. Phys. Chem.* **1989**, *93* (12), 4941−4951.
(48) Grant, J. A.; Pickup, B. T.; Nicholls, A. A smooth permittivity function for Poisson−Boltzmann solvation methods. *J. Comput. Chem.* **2001**, *22* (6), 608−640.
(49) Word, J. M.; Lovell, S. C.; Richardson, J. S.; Richardson, D. C. Asparagine and glutamine: using hydrogen atom contacts in the choice of side-chain amide orientation. *J. Mol. Biol.* **1999**, *285* (4), 1735−1747.
(50) *VIDA*, version 4.2.0; OpenEye Scientific Software, Inc., Santa Fe, NM, USA, 2012; www.eyesopen.com.
(51) *Molecular Operating Environment (MOE)*, version 2011.10; Chemical Computing Group Inc.: Montreal, Quebec, Canada, 2010.
(52) Lee, C.-J.; Liang, X.; Chen, X.; Zeng, D.; Joo, S. H.; Chung, H. S.; Barb, A. W.; Swanson, S. M.; Nicholas, R. A.; Li, Y.; Toone, E. J.; Raetz, C. R. H.; Zhou, P. Species-Specific and Inhibitor-Dependent Conformations of LpxC: Implications for Antibiotic Design. *Chem. Biol.* **2010**, *18* (1), 38−47.
(53) *OMEGA*, version 2.4.6; OpenEye Scientific Software, Inc., Santa Fe, NM, USA, 2012; www.eyesopen.com.
(54) Jakalian, A.; Jack, D. B.; Bayly, C. I. Fast, efficient generation of high-quality atomic charges. AM1-BCC model: II. Parameterization and validation. *J. Comput. Chem.* **2002**, *23* (16), 1623−1641.
(55) Tong, Y.; Claiborne, A.; Stewart, K. D.; Park, C.; Kovar, P.; Chen, Z.; Credo, R. B.; Gu, W.-Z.; Gwaltney, Ii, S. L.; Judge, R. A.; Zhang, H.; Rosenberg, S. H.; Sham, H. L.; Sowin, T. J.; Lin, N.-h. Discovery of 1,4-dihydroindeno[1,2-c]pyrazoles as a novel class of potent and selective checkpoint kinase 1 inhibitors. *Bioorg. Med. Chem.* **2007**, *15* (7), 2759−2767.
(56) Aronov, A. M.; Tang, Q.; Martinez-Botella, G.; Bemis, G. W.; Cao, J.; Chen, G.; Ewing, N. P.; Ford, P. J.; Germann, U. A.; Green, J.; Hale, M. R.; Jacobs, M.; Janetka, J. W.; Maltais, F.; Markland, W.; Namchuk, M. N.; Nanthakumar, S.; Poondru, S.; Straub, J.; ter Haar, E.; Xie, X. Structure-Guided Design of Potent and Selective Pyrimidylpyrrole Inhibitors of Extracellular Signal-Regulated Kinase (ERK) Using Conformational Control. *J. Med. Chem.* **2009**, *52* (20), 6362−6368.
(57) Wendt, M. D.; Rockway, T. W.; Geyer, A.; McClellan, W.; Weitzberg, M.; Zhao, X.; Mantei, R.; Nienaber, V. L.; Stewart, K.; Klinghofer, V.; Giranda, V. L. Identification of Novel Binding Interactions in the Development of Potent, Selective 2-Naphthamidine Inhibitors of Urokinase. Synthesis, Structural Analysis, and SAR of N-Phenyl Amide 6-Substitution. *J. Med. Chem.* **2003**, *47* (2), 303−324.
(58) *Suite 2012: Maestro*, version 9.3; Schrödinger, LLC, New York, 2012.
(59) Robin, X.; Turck, N.; Hainard, A.; Tiberti, N.; Lisacek, F.; Sanchez, J. C.; Muller, M. pROC: an open-source package for R and S + to analyze and compare ROC curves. *BMC Bioinf.* **2011**, *12*, 77.
(60) R Development Core Team (2012). *R: A language and environment for statistical computing*; R Foundation for Statistical Computing, Vienna, Austria. ISBN 3-900051-07-0; http://www.R-project.org.